CuPc Passivation of MAPbBr3 Single Crystal Surface

Ke Wang¹, Benjamin Ecker¹, Mingze Li², Jinsong Huang², and Yongli Gao^{1*}

¹Department of Physics and Astronomy, University of Rochester, Rochester, NY 14627

²Department of Applied Physical Sciences, University of North Carolina at Chapel Hill, Chapel Hill, NC, 27599

Abstract

In this study, a facile passivation for methylammonium lead bromide (MAPbBr₃) single crystal is reported. Stability against moisture and light remains the most critical demerit of perovskite materials, which is improved by depositing a 40 Å thick hydrophobic copper phthalocyanine (CuPc) layer on top of the cleaved perovskite The water and light exposure processes were monitored with X-ray surface. photoelectron spectroscopy (XPS) with precise control of the exposure time and It is found that the CuPc top layer could protect the sample from the pressure. moisture infiltration at water exposure of 10¹³ L while the non-passivated sample started to degrade at 10⁸ L. During the light exposure, CuPc also slowed down the light-induced degradation, which is supported by the elemental ratio change of metallic lead and bromine. These results are further confirmed with the morphological comparison via scanning electron microscope (SEM) and focused ion beam (FIB). Keywords: Methylammonium lead bromide, Single crystal, Stability, Copper phthalocyanine, Surface passivation.

Introduction

Organic-inorganic hybrid perovskites are considered to be an ideal candidate for the next generation solar cells as the power conversion efficiency (PCE) of perovskite solar cells (PSCs) experienced a rapid development from 3.3% in 2009 to 25.7% in 2022.[1-3] Compared to its peers, methylammonium lead halide (MAPbX₃) exhibits excellent optical and electrical properties, including high absorption coefficient, high charge carrier mobility, long carrier lifetimes, low trap density, and high photoluminescence quantum yield, which results in a strong light-harvesting ability and high efficiency in light emission and detection.[4-9] These outstanding features of MAPbX₃ have broadened its potential applications to solid state lasers, light-emitting diodes, photodetectors and gas detectors.[10-13] However, one of the biggest issue for this type of material is that it's vulnerable to almost all environmental factors such as heat, moisture, gas exposure and light irradiation.[14-23] A lot of techniques have been applied to enhance the stability of perovskites including solvent engineering, additive engineering and passivation engineering.[24] In particular, passivation techniques can decrease the efficiency loss by effective reducing charge carrier recombination and ion migration. Abdi-Jalebi et al. reported potassium iodide can fill the iodine vacancies then suppress the ion migration process.[25] Jiang et al. synthesized planar-structure PSCs with PbI₂ passivation achieving efficiency surpassing 21%, where moderate excess PbI₂ could enhance charge separation and reduce the carrier recombination at the interface. [26] Copper phthalocyanine (CuPc), a bright, crystalline, synthetic blue pigment was first used as a p-type semiconductor in

light-emitting diodes and organic solar cells for its outstanding carrier mobility and stability.[27, 28] It was introduced to PSCs as a hole transport layer (HTL), and Ke et al. fabricated PSCs with long-term thermal stability and an efficiency of 14.5% using CuPc as the HTL.[29] Qu et al. further improved the efficiency of PSCs employing CuPc derivative to 23% and maintained 96% of its initial efficiency after 3624 hours aging at 85 °C.[30] Various works have been done focusing on the device level and showed that CuPc is an ideal HTL material with long term thermal stability.[29-34] However, the effects of CuPc passivation at surface analytical level are rarely touched by the research community. Especially, as a hydrophobic material, its effects on water and light stability of perovskite have yet to be investigated.

In this paper, we report our systematic experimental investigation on the CuPc passivation effect of the *in-situ* cleaved MAPbBr₃ single crystal under water and light exposures at the surface level in an ultrahigh vacuum (UHV) system. By depositing a 40 Å thick top layer of CuPc to the MAPbBr₃ single crystal, excellent protection against water and reduced light degradation were observed. X-ray photoemission spectroscopy (XPS) was used to monitor the chemical compositional changes of the perovskite sample. Water exposure was carefully controlled and measured in Langmuir (L, 1 L = 10^{-6} Torr·s). Scanning electron microscopy (SEM) along with focused ion beam (FIB) provided both surface and bulk morphological information of the single crystal. We found that for the CuPc-passivated sample, the surface had no oxygen signals after the total 10^{13} L exposure (equivalent to 200 h), while the pristine sample started to see non-neglectable oxygen component at 10^5 L and it continued to

grow with the water exposure. It shows the water molecules were expelled from the sample surface by CuPc layer which protected the sample from water infiltration and water-induced degradation. In light exposure, the perovskite Pb decomposes into metallic Pb, and C, N, and Br decompose into volatile species and leave the surface. With CuPc passivation, there was 36.3% of total Pb converted to metallic Pb after 44 h of light exposure, while the number increased to 64.0% for the pristine crystal. Br ratio also saw a slower decay rate with the CuPc-passivated sample. Furthermore, the CuPc layer remained intact after water exposure, in contrast to almost complete desorption observed after light exposure. SEM and FIB analysis showed that the passivated sample underwent minimal changes in both surface and bulk after water exposure, with only a mild surface roughening observed compared to the pristine sample after light exposure. The results indicate that CuPc is not only an ideal thermal stable HTL material, but it can also enhance the stability of perovskite against both water and light, which could potentially expand the range of applications for CuPc.

Experimental Details

The MAPbBr3 single crystal was prepared by a solution-processed antisolvent growth method and the details can be found in ref. [35]. The single crystal sample used in this study has an average size of \sim 5 mm \times 5 mm \times 4 mm. The sample was cleaved in-situ to obtain a contamination-free pristine surface, and both the exposure and CuPc deposition processes were carried out in a vacuum system that is directly connected to the XPS analytical chamber. The XPS was operated at 10 kV and 10 mA, with a monochromatic Al K α source (1486.6 eV). Once the as-cleaved pristine sample

was measured with XPS. It was then transferred to evaporation chamber for CuPc passivation. CuPc powder was purchased from Sigma Aldrich and loaded in a tantalum boat for thermal evaporation. The evaporation rate was kept at 1 Å/min and the thickness was monitored with quartz crystal monitor (QCM).

For water exposure, the steps prior to 10⁵ L were conducted in the analytical chamber, and the remaining steps were conducted in the exposure chamber with a base pressure of 1 × 10⁻⁶ Torr. The water vapor was supplied with a distilled water tube that was connected to both XPS chamber and the exposure chamber. For light exposure, it was stored in the analytical chamber with a base pressure of 1 × 10⁻¹⁰ Torr for the entire exposure period. The excitation source was a 408 nm continuous wave laser with an intensity of 7.65 mW/mm², which is approximately seven times the sun intensity (1 mW/mm²). It was attached to a viewport of the chamber and the illuminated spot was positioned at the center of the surface. After each step, the sample was immediately transferred to the XPS chamber for XPS measurements. A microscope was mounted onto the analytical chamber to monitor the XPS measuring spot, ensuring that each measurement was taken at the same location.

After the exposure, the sample was transferred to a Zeiss Auriga SEM-FIB system in a vacuum-sealed desiccator for morphological and depth profiling. The accelerating voltage of SEM was set to 5 kV to minimize the damage from the electron beam. FIB was used to mill a $5-10~\mu m$ deep trench to investigate the effects on the bulk part. The XPS spectra were fitted with Shirley-type background and Gaussian-Lorentzian convolution. The elemental ratio of the surface was obtained by

comparing the areas of the fitted curves divided by their atomic sensitivity factors of the system.

Results and Discussion

The pristine MAPbBr3 single crystals were measured with XPS before CuPc passivation to check their initial surface composition. Their crystal quality has been confirmed with previous X-ray diffraction (XRD).[18, 20, 35] The elemental ratio of C/N/Pb/Br are 1.53/1.08/1/2.82 and 1.31/1.29/1/2.50 for water and light exposures respectively, where Pb's ratio was set as 1 to be compared with. This ratio is close to the ideal stoichiometric value. The residual reactants used in the sample growth process could be responsible for the minor excess of carbon and nitrogen present, and the insufficient Br was probably due to Br vacancies on the surface. For each exposure, we did it with pristine and CuPc-passivated samples respectively to study the effects of the CuPc passivation layer.

After the water exposures, the most noticeable variation was observed in the oxygen spectra (Figure 1). Both samples had no oxygen prior to the water exposure, showing the samples had good quality without contamination. On the pristine sample, detectable oxygen signals started appearing at 532.97 eV after 10⁵ L, and their intensity continued to increase with prolonged exposure. The peak had a binding energy (BE) shift toward higher BE region and reached 533.22 eV after 10¹³ L. This 0.25 eV shift reflects a n-doping of the surface as the Fermi level moved closer to the conduction band minimum within the bandgap. This observation is also consistent with our previous report.[20] It eventually became the dominate signal on the surface with a

ratio of 4.73, suggesting the pristine surface had absorbed considerable amount of water vapor. itionally, we learned that after 10⁸ L, water can react with perovskite, resulting in the loss of concentration of C, N, and Br. These elements become volatile species and escape from the surface. Also, water exposure caused significant roughening of the surface. [20] pntrast, the CuPc-passivated sample did not show any trace of oxygen throughout the exposure. In our precisely controlled environment, the detected oxygen was originated from water vapor, which means that water vapor could stick onto the surface of the pristine sample and kept accumulating while the hydrophobic CuPc top layer could effectively repel the water from the surface and block the reactions between water and perovskite.

The XPS core level spectra and ratio comparison of Pb 4f are shown in Figure 2. Both samples saw a small secondary Pb peak formation during the exposure, which is attributed to the formation of metallic Pb.[18] However, the formations emerged at the different stages of the exposure on two samples. The pristine sample didn't have the secondary peak when the exposure was initiated, but it showed up at 10⁴ L and continue to grow until 10¹⁰ L with a maximum ratio of 0.16, indicating the metallic Pb component made up 16% of the total Pb signal. Then it quickly dropped and eventually vanished at 10¹² L, due to the re-oxidation caused by the increasing water pressure. The transition of Pb component and the decline of C, N and Br concentrations confirm that the pristine sample was decomposed by the water exposure. On the CuPc-passivated sample, the metallic Pb emerged before the exposure started. This can be explained by the deposition of the CuPc layer, as thermal evaporated CuPc

thin films are reported to have the evaporation temperature above 300 °C.[36] refore, the heated CuPc molecules could cause thermal-induced degradation when they landed on the perovskite surface, resulting in the formation of metallic Pb. Different from the pristine sample, the metallic Pb component peaked at 10³ L and vanished at 10⁷ L on the CuPc-passivated sample. It shows that after initial thermal degradation caused by hot CuPc molecules, water exposure didn't further decompose the surface, as CuPc layer served as a protection layer. Pd 4f XPS spectra also showed that the Pb peak shifted ~0.45 eV toward the lower BE region after the CuPc passivation, then slowly moved back to higher BE with the water exposure. The BE movement suggests that the pristine surface was p-doped by CuPc and then gradually n-doped by water. This p-doping effect was also reported in other literatures.[37-39] The discussion above revealed that CuPc top layer can protect the perovskite surface from water-induced degradation by effectively repel the water molecules from the surface.

Light irradiation is another major challenge for perovskite stability and we performed precisely controlled light exposure on CuPc-passivated perovskite to investigate its effect on the stability of the sample. Figure 3 shows a significant change, where the metallic Pb component is much larger than that observed in the previous water exposure. Both samples started to have metallic Pb peak after the light exposure was initiated, indicating the perovskite Pb decomposed into metallic Pb as a result of light-induced degradation. The metallic Pb quickly grew and became the dominate component after 10 hours light exposure on pristine surface and eventually made up 65% of the total Pb signal. In contrast, metallic Pb showed a much slower

and mild growth on the CuPc-passivated surface with a final composition of 36% of the total Pb concentration. This value is equivalent to that of only 8 hours of light exposure on the pristine surface. The perovskite Pb peak was located at 138.25 eV and began to shift toward lower BE region when exposure started, indicating a p-doping of the pristine surface. This can be explained by either a decrease in the number of n-type traps on the surface due to photogenerated charge carriers, or the reversible creation of p-type traps caused by light exposure.[40] After 2 hours exposure, the peaks gradually shifted back to higher BEs and settled at 138.47 eV. The overall BE movement suggests a n-doping of the pristine surface due to halide reduction and metallic Pb works as p-dopant, which agrees well with existing literature.[41, 42] The CuPc-passivated surface also showed a similar pattern, the difference is the initial p-doping was mostly caused by CuPc. Pb and other core levels (Br, and VBM showed a ~0.42 eV shift to lower BE region, which is comparable to that in water exposure. Again, the consistent result confirmed CuPc worked as a p-dopant.

The decreasing trend in Br ratio, as shown in Figure 4b icates that the sample decomposed into Br₂, which is a volatile substance that left the surface. The final Br concentrations were 21% and 37% of their initial values for pristine and CuPc-passivated surface respectively. The milder loss of Br in the CuPc-passivated surface suggests a less severe degradation induced by light exposure. The concentration loss of perovskite C, N and Br caused a metallic Pb rich surface which n-doped the surface. The presence of CuPc passivation layer could inhibit the escape of decomposed volatile species and impede the degradation of perovskite Pb into metallic Pb, therefore protect

the surface from further damage.

By comparing the effects of water and light exposures, we observed that the CuPc passivation layer provided differing degrees of protection. While CuPc demonstrated its ability to shield the MAPbBr3 single crystal from water- and light-induced degradation, the elemental ratios of C, N, and Cu from CuPc exhibited distinctive behaviors. As shown in Figure 5, in the water-exposed sample, the ratios fluctuated as water exposure increased. The N and Cu ratios remained similar to their initial values, while C gained approximately 37%, which is comparable to that in the pristine surface. This can be attributed to the formation of a hydrocarbon complex.[20] suggests that the CuPc top layer remained mostly intact even after 12 days of water exposure in the UHV chamber. Surprisingly, in the light-exposed sample, all ratios quickly dropped as soon as the exposure started, and eventually settled at approximately 5% of their initial value. This indicates that the light exposure caused laser desorption of the CuPc passivation layer, eventually exposing the underlying perovskite surface. The comparison of XPS survey scans (Figure S1) confirms once again the different behaviors of the CuPc passivation layer after water and light exposures. In waterexposed sample, the survey scans remained almost identical before and after the exposure, as there was no new peaks or absence of peaks. In contrast, during light exposure, the survey scans for the as-treated and non-exposed regions were almost the same, while the light-exposed region exhibited the reappearance of Br and Pb signals the underlying perovskite. This further confirms that laser irradiation caused the CuPc layer to be optically desorbed from the surface, which subsequently exposed the

underlying perovskite. The varying responses of the CuPc layer to different exposures result in differences in its protective performance on perovskites.

We also conducted SEM and FIB measurements on our samples to investigate its morphological changes on both surfaces and bulk parts. The as-treated sample showed a clear and featureless surface, confirming CuPc formed a smooth and uniform top layer via thermal evaporation. FIB milled trench showed the bulk part of the sample was pristine to begin with the morphological changes occurred after water and light exposure, but they were more moderate compared to these non-passivated samples.[18] The water exposed sample demonstrated a mild-roughened surface, but the bulk part remains integrity. The surface was still more uniform than that of the non-passivated vacuum exposed sample, which confirms that CuPc could protect the sample from water infiltration and the morphological change was merely due to degassing in the UHV chamber. For the light exposed sample, there were small bumps formed across the surface. It could be attributed to metallic Pb aggregation. Even thought, its surface features were substantially smaller and more uniform than the nonpassivated sample.[18] In contrast to the non-passivated light-exposed sample, the CuPc-passivated sample did not exhibit the formation of cracks and voids in its bulk This indicates that the top CuPc layer can prevent light penetration into the bulk and suppress volatile substance leaving the surface, thereby protecting the bulk part of the crystal. It's worth noting that not all hydrophobic organic materials can protect the underlying substrate. Rubrene, for example, is even worse at water protection as it cannot form a uniform layer. (Figure S2) As a result, it repels water towards the exposed perovskite region, leading to even higher water concentration on the perovskite surface, which ultimately results in more severe degradation.

Conclusion

In this study, we examined the effects of the CuPc passivation layer on MAPbBr3 single crystal under water and light exposures. Our findings indicate that a 40 Å thick CuPc top layer can effectively protect the perovskite against water exposure by repelling water molecules from the surface. However, it can only delay the light-induced degradation of perovskite by approximately 36 hours. The differing protective abilities can be attributed to the distinct behaviors of the CuPc layer, which was found to be desorbed by light, while remaining mostly intact after exposure to water. SEM and FIB results revealed that CuPc forms a uniform and featureless layer, resulting in significantly milder morphological changes on both the perovskite surfaces and bulk parts, in comparison to those exposed to water and light without CuPc. Our investigation demonstrates that CuPc can not only improve the thermal stability of perovskites but also enhance their water and photostability, thereby expanding the methods for enhancing the stability of perovskites and contributing to the development of high-performance perovskite devices.

Acknowledgement

The work receives financial support from National Science Foundation (Grant # DMR-1903962). B.E. acknowledges Hooker Dissertation Fellowship from the University of Rochester. The authors would like to thank URnano center at University of Rochester for technical support with SEM, FIB measurements.

Conflicts of Interest

The authors declare no conflict of interest.

Figures:

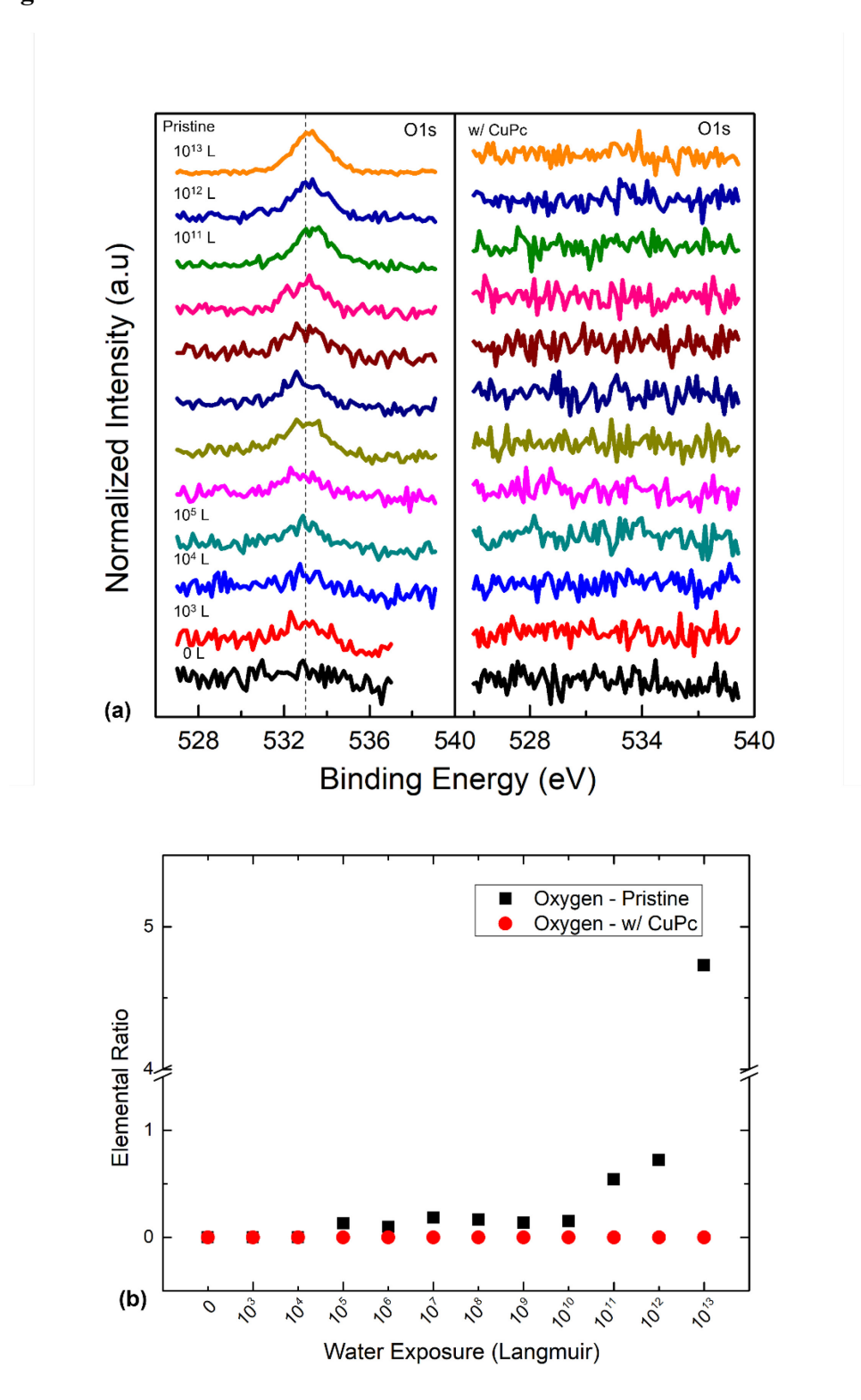


Figure 1. (a) Evolutions of O 1s XPS spectra comparison of pristine and CuPcpassivated perovskites with increasing water exposure. (b) Oxygen ratio trend comparison for the pristine and the CuPc-passivated perovskites.

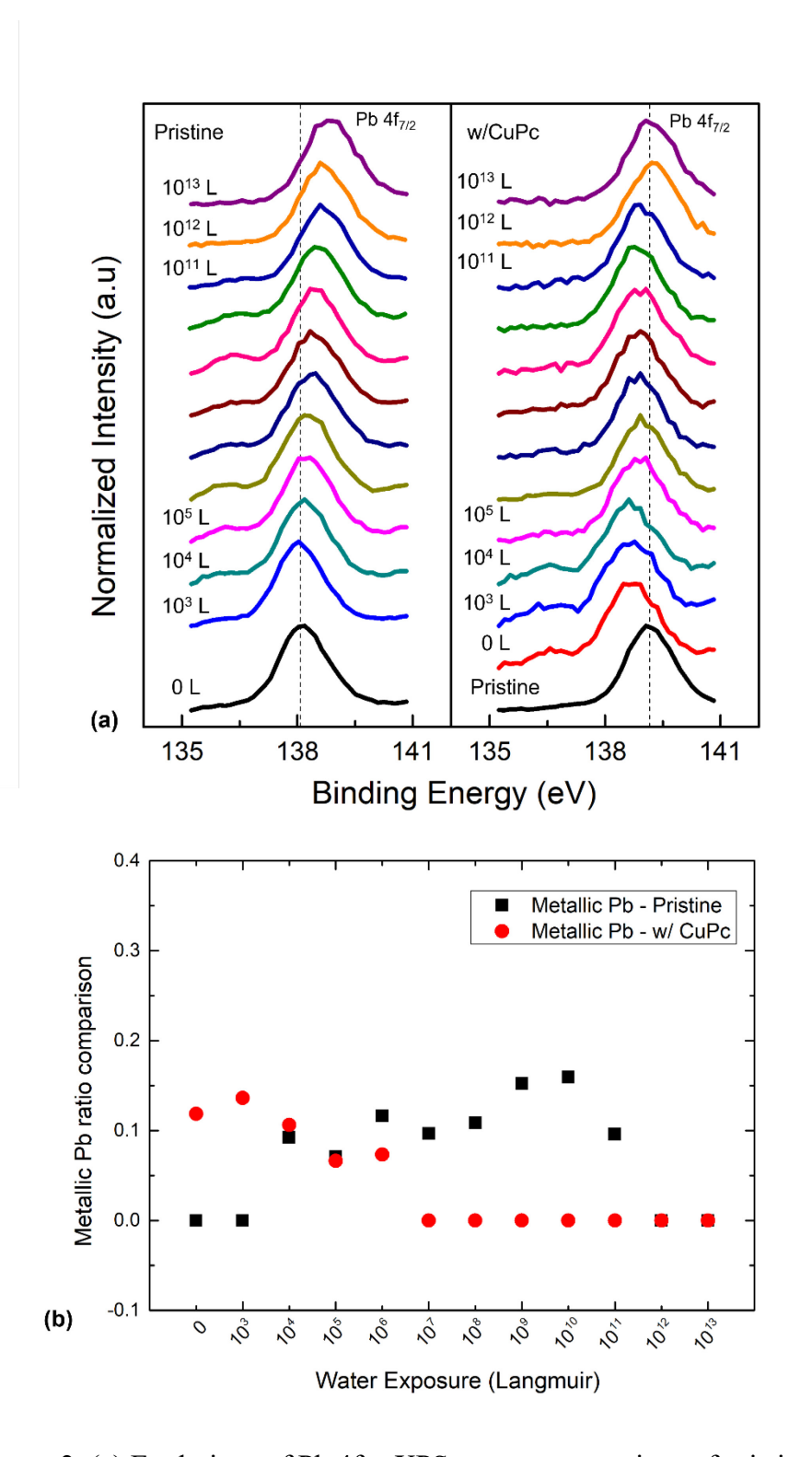


Figure 2. (a) Evolutions of Pb $4f_{7/2}$ XPS spectra comparison of pristine and CuPc-passivated perovskites with increasing water exposure. (b) Metallic Pb ratio trend comparison for pristine and CuPc-passivated perovskites with light exposure.

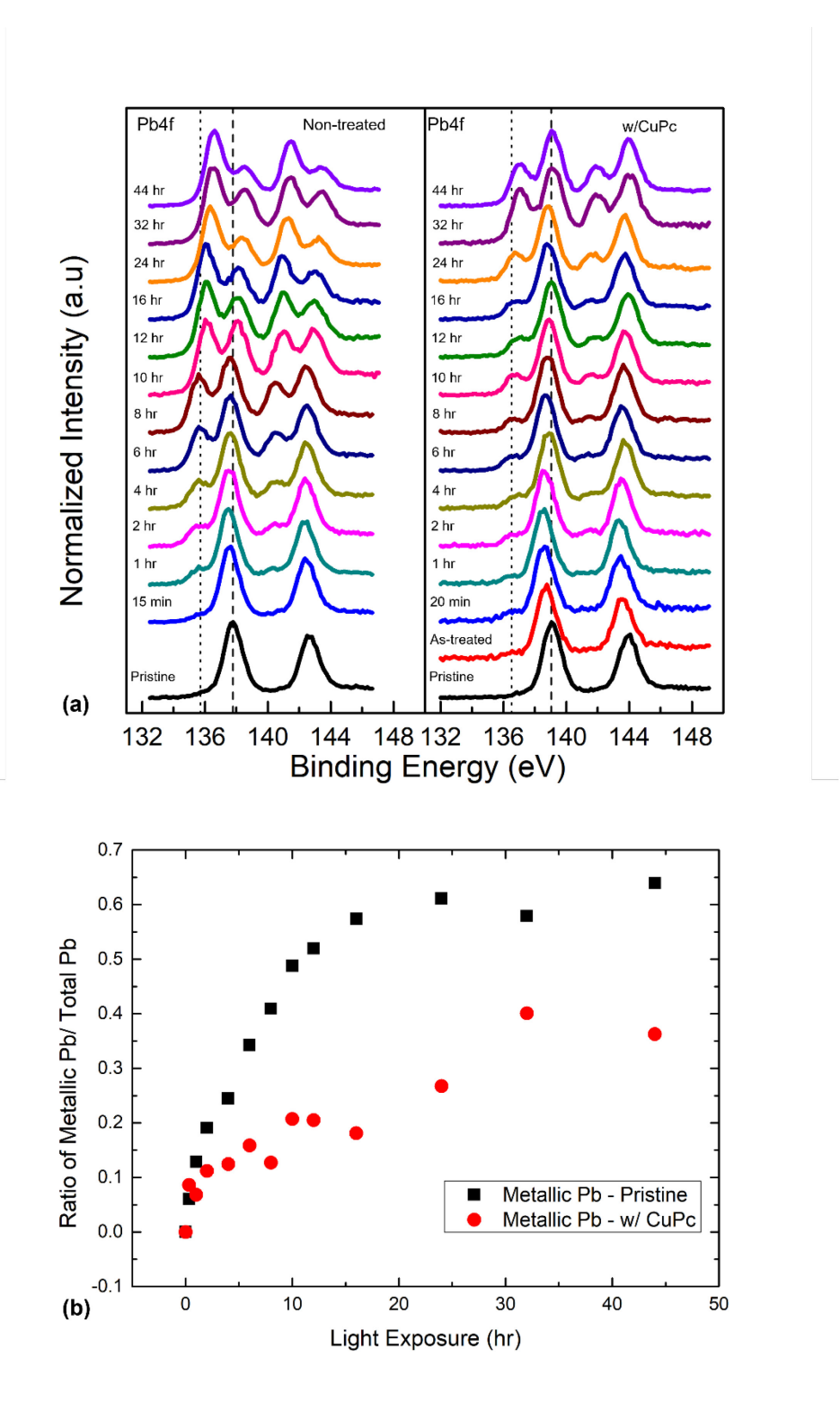


Figure 3. (a) Evolutions of Pb 4f XPS spectra comparison of pristine and CuPc-passivated perovskites with increasing light exposure. (b) Metallic Pb ratio trend comparison for pristine and CuPc-passivated perovskites with light exposure.

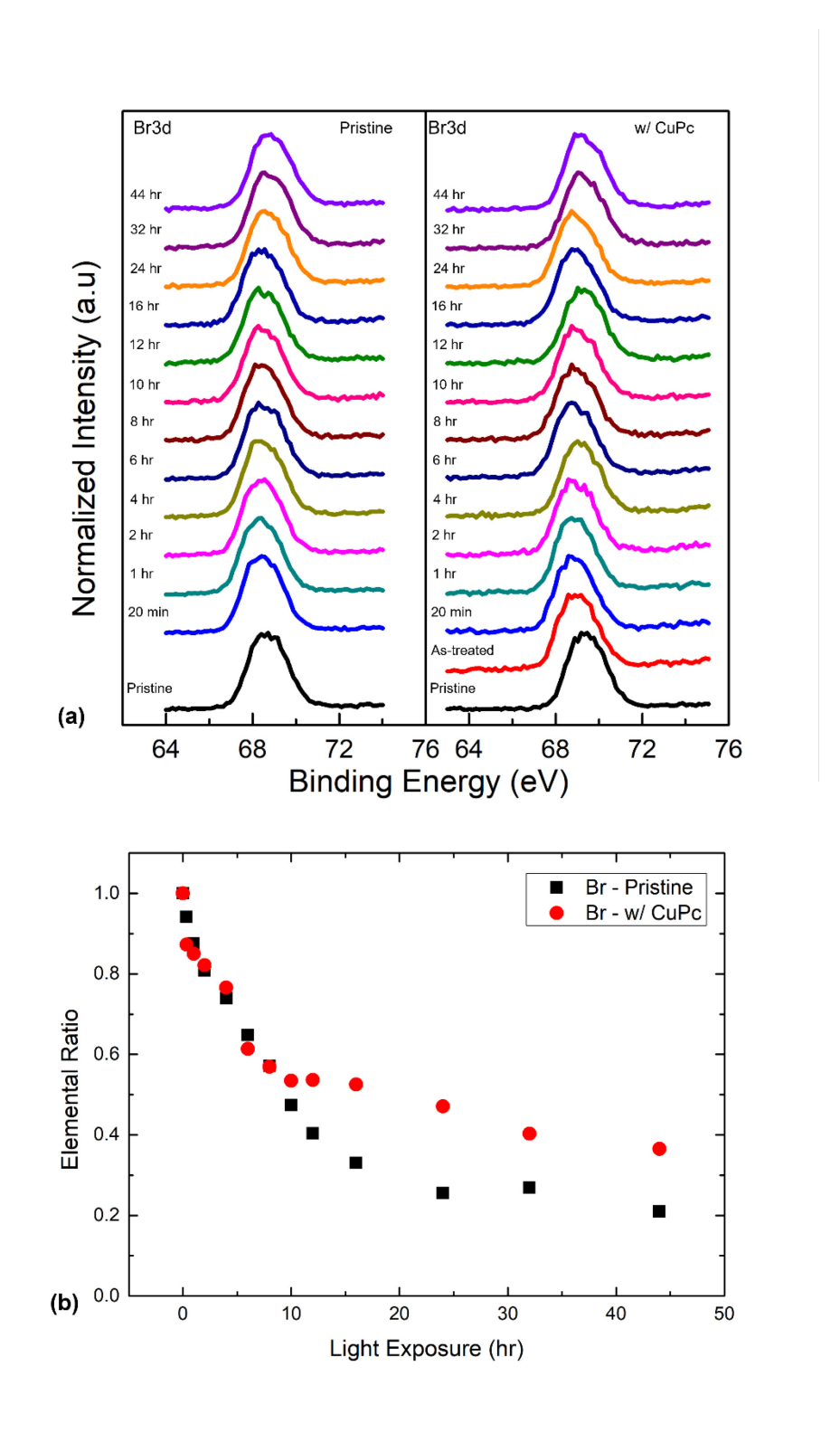


Figure 4. (a) Evolutions of Br 3d XPS spectra comparison of pristine and CuPc-passivated perovskites with increasing light exposure. (b) Metallic Pb ratio trend comparison for pristine and CuPc-passivated perovskites with light exposure.

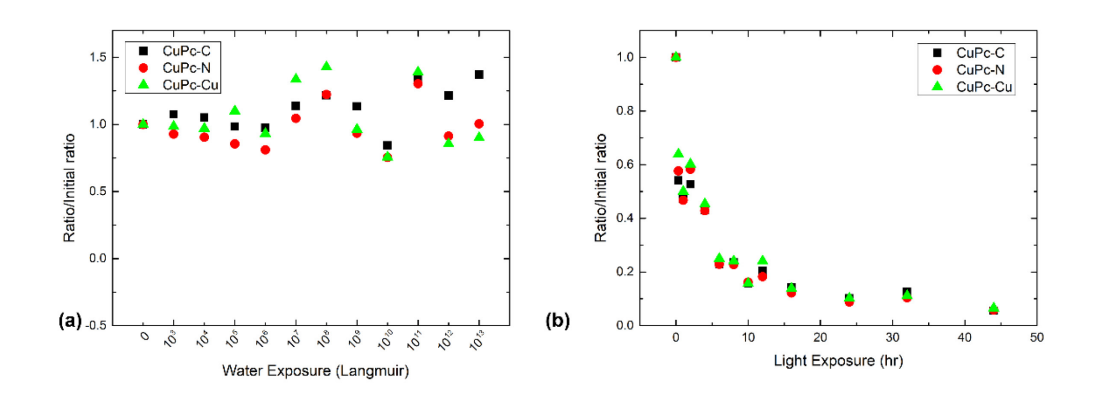


Figure 5. Carbon, nitrogen, bromide ratio trend of CuPc passivation layer for (a) water exposure and (b) light exposure.

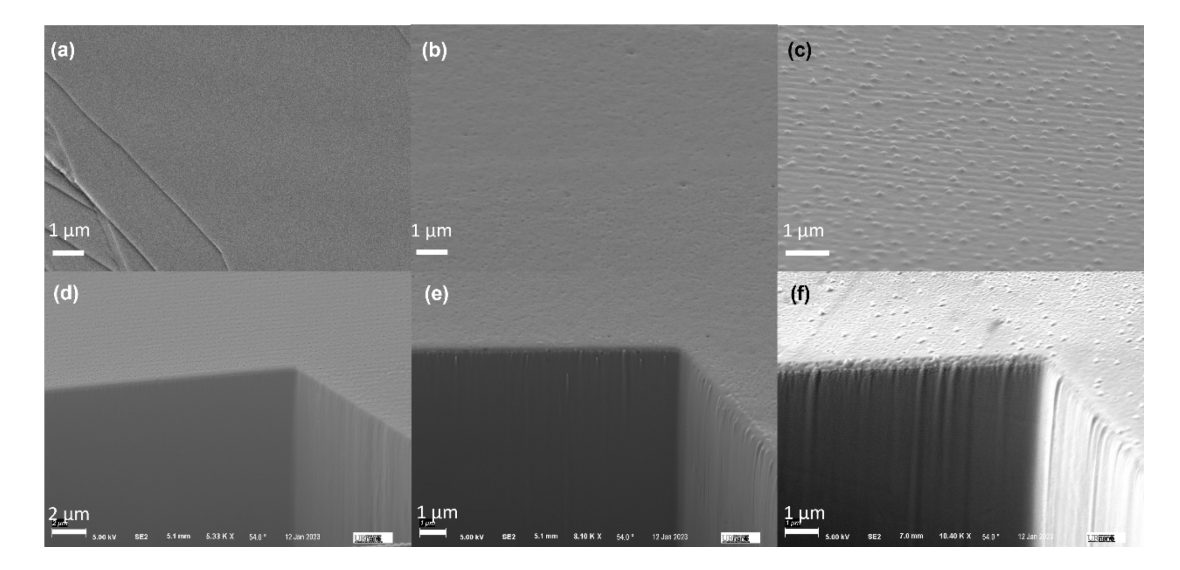


Figure 6. (a-c) SEM image of the surface of the freshly passivated, water exposed and light exposed samples respectively. (d-f) FIB milled trenches for the freshly passivated, water exposed and light exposed samples respectively. The FIB milled trench of the selected region revealed about 6-10 µm deep into the material.

Reference

- 1. Kojima, A., et al., *Organometal Halide Perovskites as Visible-Light Sensitizers for Photovoltaic Cells.* Journal of the American Chemical Society, 2009. **131**(17): p. 6050-6051.
- 2. Snaith, H.J., *Perovskites: The Emergence of a New Era for Low-Cost, High-Efficiency Solar Cells.* The Journal of Physical Chemistry Letters, 2013. **4**(21): p. 3623-3630.
- 3. Best Research-Cell Efficiency Chart (National Renewable Energy Laboratory), available at https://www.nrel.gov/pv/cell-efficiency.html.
- 4. Sheng, R., et al., *Methylammonium lead bromide perovskite-based solar cells by vapor-assisted deposition.* The Journal of Physical Chemistry C, 2015. **119**(7): p. 3545-3549.
- 5. Wei, H., et al., *Sensitive X-ray detectors made of methylammonium lead tribromide perovskite single crystals.* Nature Photonics, 2016. **10**(5): p. 333-339.
- 6. Kim, H.-S., et al., *Mechanism of carrier accumulation in perovskite thin-absorber solar cells.* Nature communications, 2013. **4**(1): p. 2242.
- 7. Droseros, N., et al., *Origin of the enhanced photoluminescence quantum yield in MAPbBr3* perovskite with reduced crystal size. ACS energy letters, 2018. **3**(6): p. 1458-1466.
- 8. Wang, K., et al., *Evaporation of Methylammonium lodide in Thermal Deposition of MAPbl3.* Nanomaterials, 2021. **11**(10): p. 2532.
- 9. Wang, K., B. Ecker, and Y. Gao, *Angle-Resolved Photoemission Study on the Band Structure of Organic Single Crystals*. Crystals, 2020. **10**(9): p. 773.
- 10. Xing, G., et al., *Low-temperature solution-processed wavelength-tunable perovskites for lasing*. Nature materials, 2014. **13**(5): p. 476-480.
- 11. Tan, Z.-K., et al., *Bright light-emitting diodes based on organometal halide perovskite.*Nature nanotechnology, 2014. **9**(9): p. 687-692.
- 12. Dou, L., et al., *Solution-processed hybrid perovskite photodetectors with high detectivity.*Nature communications, 2014. **5**(1): p. 5404.
- 13. Fang, H.-H., et al., *Ultrahigh sensitivity of methylammonium lead tribromide perovskite single crystals to environmental gases.* Science advances, 2016. **2**(7): p. e1600534.
- 14. Brunetti, B., et al., *On the thermal and thermodynamic (in) stability of methylammonium lead halide perovskites.* Scientific reports, 2016. **6**(1): p. 1-10.
- 15. Alberti, A., et al., *Revealing a discontinuity in the degradation behavior of CH3NH3Pbl3 during thermal operation.* The Journal of Physical Chemistry C, 2017. **121**(25): p. 13577-13585.
- 16. Christians, J.A., P.A. Miranda Herrera, and P.V. Kamat, *Transformation of the excited state and photovoltaic efficiency of CH3NH3Pbl3 perovskite upon controlled exposure to humidified air.* Journal of the American Chemical Society, 2015. **137**(4): p. 1530-1538.
- 17. Kye, Y.-H., et al., *Critical role of water in defect aggregation and chemical degradation of perovskite solar cells.* The journal of physical chemistry letters, 2018. **9**(9): p. 2196-2201.
- 18. Ecker, B.R., et al., *Intrinsic Behavior of CH3NH3PbBr3 Single Crystals under Light Illumination*. Advanced Materials Interfaces, 2018. **5**(23).
- 19. Wang, C., et al., *Degradation of Co-Evaporated Perovskite Thin Film in Air.* Chemical Physics Letters, 2016. **649**: p. 151-155.
- 20. Wang, C., et al., *Environmental Surface Stability of the MAPbBr3 Single Crystal.* The Journal of Physical Chemistry C, 2018. **122**(6): p. 3513-3522.

- 21. Li, Y., et al., *Degradation by Exposure of Coevaporated CH3NH3Pbl3 Thin Films*. The Journal of Physical Chemistry C, 2015. **119**(42): p. 23996-24002.
- 22. Li, Y., et al., *Light-Induced Degradation of CH3NH3Pbl3 Hybrid Perovskite Thin Film.* The Journal of Physical Chemistry C, 2017. **121**(7): p. 3904-3910.
- 23. Wang, K., B. Ecker, and Y. Gao, *Photoemission Studies on the Environmental Stability of Thermal Evaporated MAPbl3 Thin Films and MAPbBr3 Single Crystals.* Energies, 2021. **14**(7): p. 2005.
- 24. Mahapatra, A., et al., *Recent progress in perovskite solar cells: challenges from efficiency to stability.* Materials Today Chemistry, 2022. **23**: p. 100686.
- 25. Abdi-Jalebi, M., et al., *Maximizing and stabilizing luminescence from halide perovskites with potassium passivation.* Nature, 2018. **555**(7697): p. 497-501.
- 26. Jiang, Q., et al., *Planar structure perovskite solar cells with efficiency beyond 21%.* Advanced materials, 2017. **29**(46): p. 1703852.
- 27. Yu, W.-L., et al., *Hole-injection enhancement by copper phthalocyanine (CuPc) in blue polymer light-emitting diodes.* Journal of Applied Physics, 2001. **89**(4): p. 2343-2350.
- 28. Xue, J., et al., *4.2% efficient organic photovoltaic cells with low series resistances.* Applied Physics Letters, 2004. **84**(16): p. 3013-3015.
- 29. Ke, W., et al., *Efficient fully-vacuum-processed perovskite solar cells using copper phthalocyanine as hole selective layers.* Journal of Materials Chemistry A, 2015. **3**(47): p. 23888-23894.
- 30. Qu, G., et al., *Dopant-Free Phthalocyanine Hole Conductor with Thermal-Induced Holistic Passivation for Stable Perovskite Solar Cells with 23% Efficiency.* Advanced Functional Materials, 2022. **32**(41): p. 2206585.
- 31. Yang, G., et al., *A facile molecularly engineered copper (II) phthalocyanine as hole transport material for planar perovskite solar cells with enhanced performance and stability.* Nano Energy, 2017. **31**: p. 322-330.
- 32. Zhang, F., et al., *Boosting the efficiency and the stability of low cost perovskite solar cells by using CuPc nanorods as hole transport material and carbon as counter electrode.* Nano Energy, 2016. **20**: p. 108-116.
- 33. Duong, T., et al., *Perovskite solar cells employing copper phthalocyanine hole-transport material with an efficiency over 20% and excellent thermal stability.* ACS Energy Letters, 2018. **3**(10): p. 2441-2448.
- 34. Kim, Y., et al., *Engineering interface structures between lead halide perovskite and copper phthalocyanine for efficient and stable perovskite solar cells.* Energy & Environmental Science, 2017. **10**(10): p. 2109-2116.
- 35. Wei, H., et al., *Sensitive X-ray detectors made of methylammonium lead tribromide perovskite single crystals.* Nature Photonics, 2016. **10**(5): p. 333-339.
- 36. Liu, F., et al., *Controllable fabrication of copper phthalocyanine nanostructure crystals.* Nanotechnology, 2015. **26**(22): p. 225601.
- 37. Leyva Esqueda, M., et al., *Cupc: effects of its doping and a study of its organic-semiconducting properties for application in flexible devices.* Materials, 2019. **12**(3): p. 434.
- 38. Hein, C., et al., *Engineering the electronic structure of the CuPc/BPE-PTCDI interface by WO3 doping of CuPc.* physica status solidi (a), 2009. **206**(12): p. 2757-2762.
- 39. Chen, W., et al., Surface transfer doping of semiconductors. Progress in Surface Science,

- 2009. **84**(9-10): p. 279-321.
- 40. Hoke, E.T., et al., *Reversible photo-induced trap formation in mixed-halide hybrid perovskites for photovoltaics.* Chemical Science, 2015. **6**(1): p. 613-617.
- 41. Xie, H., et al., *Effects of precursor ratios and annealing on electronic structure and surface composition of CH3NH3Pbl3 perovskite films.* The Journal of Physical Chemistry C, 2016. **120**(1): p. 215-220.
- 42. Wang, Q., et al., *Qualifying composition dependent p and n self-doping in CH3NH3Pbl3.*Applied Physics Letters, 2014. **105**(16): p. 163508.